Available online at www.sciencedirect.com

SCIENCE DIRECT

Journal of Power Sources 156 (2006) 455–460

JOURNAL OF POWER SOURCES

www.elsevier.com/locate/jpowsour

Short communication

Development and testing of anode-supported solid oxide fuel cells with slurry-coated electrolyte and cathode

R. Muccillo[a,*], E.N.S. Muccillo[a], F.C. Fonseca[a], Y.V. França[a], T.C. Porfirio[a], D.Z. de Florio[b], M.A.C. Berton[c], C.M. Garcia[c]

[a] Centro de Ciência e Tecnologia de Materiais, Instituto de Pesquisas Energéticas e Nucleares, C.P. 11049, Pinheiros, S. Paulo, SP 05422-970, Brazil

[b] Instituto de Química, UNESP, R. Prof. Francisco Degni s/n, Araraquara, SP 14801-970, Brazil

[c] Instituto de Tecnologia para o Desenvolvimento, DPMA, C.P. 19067, Curitiba, PR 81531-980, Brazil

Received 19 April 2005; received in revised form 14 June 2005; accepted 17 June 2005
Available online 18 August 2005

Abstract

A laboratory setup was designed and put into operation for the development of solid oxide fuel cells (SOFCs). The whole project consisted of the preparation of the component materials: anode, cathode and electrolyte, and the buildup of a hydrogen leaking-free sample chamber with platinum leads and current collectors for measuring the electrochemical properties of single SOFCs. Several anode-supported single SOFCs of the type (ZrO_2:Y_2O_3 + NiO) thick anode/(ZrO_2:Y_2O_3) thin electrolyte/($La_{0.65}Sr_{0.35}MnO_3$ + ZrO_2:Y_2O_3) thin cathode have been prepared and tested at 700 and 800 °C after in situ H_2 anode reduction. The main results show that the slurry-coating method resulted in single-cells with good reproducibility and reasonable performance, suggesting that this method can be considered for fabrication of SOFCs.

Keywords: Solid oxide fuel cells; Solid electrolyte; Anode; Cathode; Impedance spectroscopy

1. Introduction

Fuel cells (FC) are considered one of the important power generation technologies for the future due to the ability to directly and efficiently convert chemical energy to electrical energy [1]. Among the different FC technologies, the solid oxide fuel cell (SOFC) has attracted a great deal of attention due to its high efficiency, variety of usable fuels and wide range of power generation applications [2]. The SOFC can use hydrocarbon fuels to produce electrical power with high efficiency suggesting future developments for stationary and portable applications. A SOFC generates electricity through the reduction of oxygen to O^{2-} ions at the cathode, transfer of the anions through an electrolyte that is an electronic insulator (usually cubic yttria-stabilized zirconia; YSZ), and finally by the oxidation of the fuel with O^{2-} ions at the anode. The solid oxide fuel cells operating at high temperatures (800–1000 °C) combine the benefits of environmentally benign power generation with fuel flexibility. Various designs of high temperature solid oxide fuel cells have been put into operation in a laboratory scale, the most common being the tubular, the monolithic and the planar designs [3].

Concerning the planar design, the anode-supported SOFCs have as main advantage the substantially lower ohmic resistance of the electrolyte, and consequently the lower operation temperature [4–9]. As a consequence, conventional metal interconnectors could be used at low manufacturing costs. In this SOFC, a relatively thick porous anode is used to provide structural support for the assembly. The anode-supported cells are usually fabricated by (i) sintering the anode precursor NiO + ZrO_2:8 mol% Y_2O_3, (ii) coating the anode with a thin YSZ electrolyte and firing in the

* Corresponding author. Tel.: +55 11 38169343; fax: +55 11 38169343.
E-mail addresses: muccillo@usp.br (R. Muccillo), enavarro@ipen.br (E.N.S. Muccillo), cfonseca@ipen.br (F.C. Fonseca), dzflorio@posgrad.iq.unesp.br (D.Z. de Florio), berton@lactec.org.br (M.A.C. Berton), garcia@lactec.org.br (C.M. Garcia).

0378-7753/$ – see front matter © 2005 Elsevier B.V. All rights reserved.
doi:10.1016/j.jpowsour.2005.06.021

1400–1500 °C range, (iii) coating the electrolyte thin film with the cathode ($La_{1-x}Sr_xMnO_3$, lanthanum strontium manganite; LSM) and (iv) firing the single-cell at approximately 1200 °C. Several techniques have been applied for the fabrication of anode-supported single SOFCs, resulting in different microstructures and performances. However, a simple and low-cost fabrication method has not been established and several different techniques have been considered [2,10].

One of the ideas of this paper is to show that Brazil has a great potential for establishing a national program of development of solid oxide fuel cells, the country has one of the most important deposits of minerals for obtaining ceramic grade zirconium oxide with low silica content [11], the basic material for the fabrication of solid electrolytes for solid oxide fuel cells. Brazil has also very large deposits of monazitic sand, which are basic mineral resources for obtaining lanthanum oxide, yttrium oxide and rare earth oxides. After chemical processing for separation and purification, ceramic grade zirconium oxide with <300 ppm silica content and 99.9% yttrium and lanthanum oxides are produced at IPEN. Moreover, the country has a long tradition on developing alternative fuels and renewable sources [12]. Since the seventies, ethanol has been produced in large quantities either for powering vehicles or for export. Research on SOFC development using ethanol as hydrogen source may be considered a primary challenge.

In this paper, we report the evaluation of the main parameters of a single solid oxide fuel cell using ceramic materials chemically processed at IPEN to fabricate the anode, the cathode and the electrolyte components. We should point out that to put into operation even a single SOFC is not an easy task. Besides the requirements of the main component materials: anode, electrolyte and cathode, there are other challenges to overcome, related to the peripherals of the single-cell: terminal leads, current collector, hydrogen leak-proof anode side reservoir with a suitable sealant, fuel and oxidant flow control, etc. The confirmation of the success of the development here presented is the reduction of the anode, the open cell voltage and the polarization data collected at high temperatures using hydrogen as fuel and air as oxidant. The detailed preparation of the single-cell components and the collected data are here reported.

2. Experimental

The preparation and characterization of anode-supported single SOFCs are described below.

The anode support was prepared by thoroughly mixing ZrO_2:8 mol% Y_2O_3 to nickel oxide (40/60 vol.%) in an agate mortar, adding 0.15 g of polyvinyl alcohol in 90 vol.% water solution. The slurry was dried overnight at room temperature, cold-pressed under 25 MPa in a 25 mm diameter cylindrical die and pre-sintered at 800 °C at 5 °C min^{-1} heating and cooling rates. Care should be taken for choosing appropriate particle average size and distribution as well as sintering conditions [13]. The YSZ powders were either from Tosoh Corp. (13.4 $m^2\,g^{-1}$ specific surface area) or from IPEN (∼150 $m^2\,g^{-1}$ specific surface area, prepared by co-precipitating zirconium oxychloride and yttrium nitrate obtained from hydrous zirconium hydroxide and yttrium oxide also synthesized at IPEN) [14].

The ∼1 mm thick pre-sintered YSZ–NiO anode is used as the support for the YSZ solid electrolyte. The slurries were prepared by mixing 1.5 g of ZrO_2:8 mol% Y_2O_3 and 0.04 g sodium hexametaphosphate (deflocculating agent) to the solvents butanol and cyclohexane, 2 mL of each. Afterwards, two drops of polyethylene glycol and 0.08 g polyvinyl butyral organic binders were added under continuous stirring for adjusting the viscosity in a trial and error basis to get uniform and suitable thickness by hand brushing layers onto the anode. The half-cell was dried at room temperature overnight before co-firing at 1400 °C for 1 h, 5 °C min^{-1} heating and cooling rates, to produce a homogenous and dense YSZ layer on the anode.

The LSM cathode powders were prepared by solid-state reaction among lanthanum oxide produced at IPEN, and commercial (reagent grade) strontium carbonate and manganese oxide, both from VETEC, Brazil. Mixing and heating at 1300 °C/1 h (5 °C min^{-1} heating and cooling rates) for three times with intermediate grindings in an agate mortar resulted in single phase $La_{0.65}Sr_{0.35}MnO_3$. Slurries of these powders were prepared by mixing to YSZ (50/50 wt.%) in an agate mortar, adding 0.15 g polyvinyl alcohol per 1 mL distilled water. The viscosity was adjusted to get uniform and suitable thickness deposits over the solid electrolyte following the same procedure applied for depositing the electrolyte layer. The single-cell was then fired to 1200 °C for 2 h at 3 °C min^{-1} heating and cooling rates to avoid warping, evidenced by the homogeneous partially sintered layer and mechanical integrity.

X-ray diffraction (XRD) measurements of all powder specimens, sintered pellets, electrolyte coating onto sintered anode, cathode coating onto electrolyte and anode support after cell test were carried out in a Bruker-AXS diffractometer operating at 40 kV–40 mA in a θ–2θ Bragg–Brentano configuration with Cu Kα radiation. Scanning electron microscopy (SEM) observations of fractured cross-sections were carried out in a LEO440I Oxford microscope using either secondary or backscattered electrons.

A single-cell test chamber was designed and set up for electrical measurements up to 1000 °C, see Fig. 1. It consists of a programmable vertical resistive split furnace with a sample chamber made of high alumina and quartz tubes, and platinum meshes and wires as terminal leads. For single-cell testing, platinum mesh was used as current collector and Demetron 308A (Degussa, Hanau, Germany) platinum paste was used to attach the platinum mesh to both the anode and the cathode. The sealing of the anode compartment was done by using a ring shaped pyrex piece pressed by an alumina tube and heated to 800 °C (10 °C min^{-1}) for softening. Pressurized air was inserted in the cell for checking gas tightness.

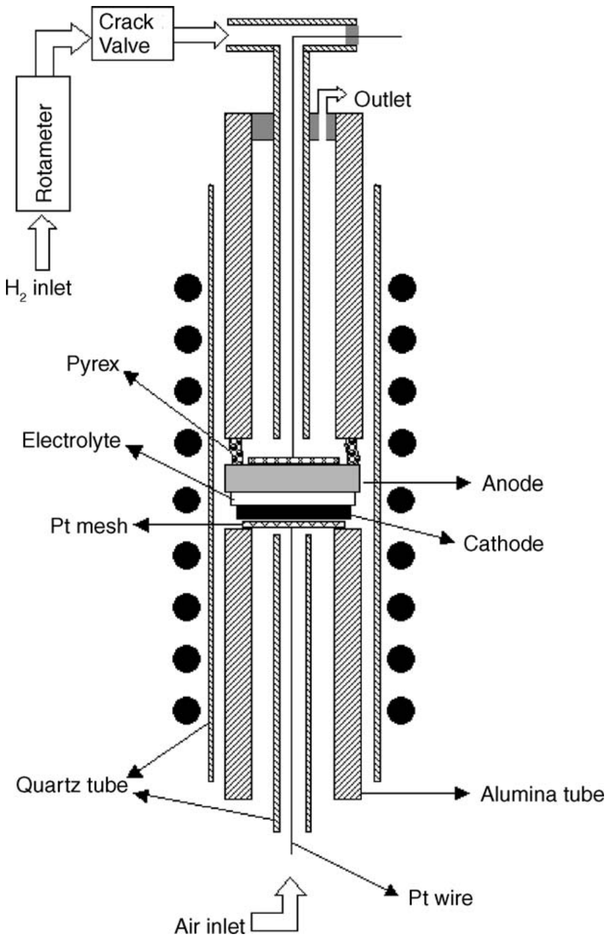

Fig. 1. Schematic drawing of the anode-supported SOFC single-cell.

The reduction of nickel oxide to nickel was achieved by heating under hydrogen gas from 600 °C to the temperature of cell testing (in the 700–800 °C range). The hydrogen gas from the cylinder supply located outside the laboratory flows through a rotameter and a crack valve, for safety purposes.

Open circuit voltage impedance spectroscopy measurements were performed in the 0.1 Hz–1 MHz frequency range at temperatures in the 700–800 °C range with amplitude signal 50 mV. The current–voltage (*I*–*V*) curves were obtained in the same temperature range. Both experiments were carried out with a Parrstat 2263 potentiostat–galvanostat. In all the electrical measurements, the internal resistance associated to the test system leads and connections were corrected.

3. Results and discussion

The single-cell components were analyzed by XRD, as shown in Fig. 2. The X-ray patterns reveal that both electrodes and the electrolyte have the desired crystalline phases and no significant spurious phases were detected.

The single SOFCs were analyzed by scanning electron microscopy. A cross-sectional image of a typical anode-supported cell is shown in Fig. 3. The thickness of the dense electrolyte and porous cathode layers was evaluated as ∼70 and ∼90 μm, respectively. In addition, the electrode/electrolyte interfaces exhibit a good homogeneity and interlayer adhesion. The anode precursor layer shows a relatively dense microstructure due to the absence of pore formers addition during the preparation step. However, the oxygen release during the reduction of NiO is expected to promote some porosity in the anode [15].

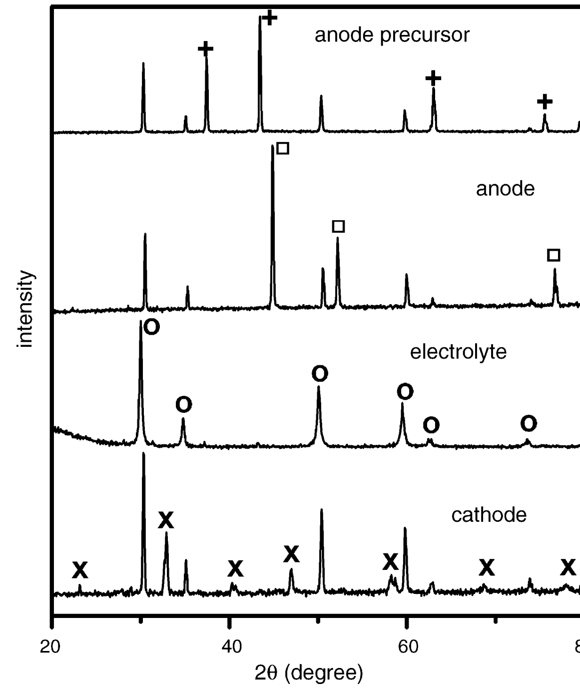

Fig. 2. X-ray diffraction patterns of the main components of the SOFC; from top to bottom: yttria-stabilized zirconia + nickel oxide (40/60 vol.%) anode precursor; yttria-stabilized zirconia + nickel anode support after cell test, yttria-stabilized zirconia solid electrolyte and lanthanum strontium manganite + yttria-stabilized zirconia (50/50 wt.%) cathode. Indexing of main reflections: (o) YSZ, (+) NiO, (□) Ni and (×) LSM.

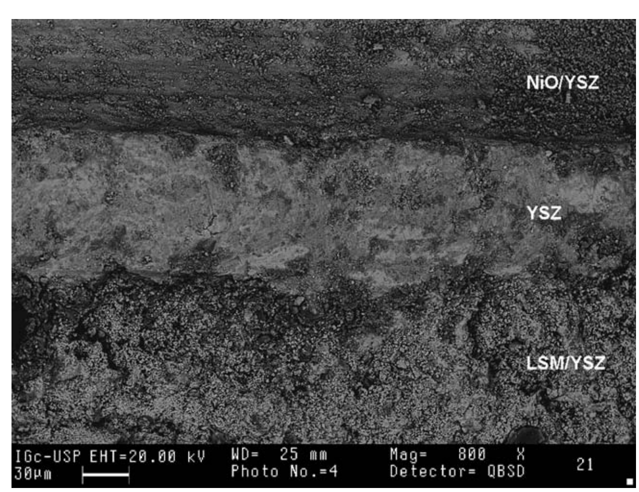

Fig. 3. Scanning electron microscopy micrograph of the cross-section of single anode-supported SOFC with slurry-coated electrolyte and cathode, before anode reduction.

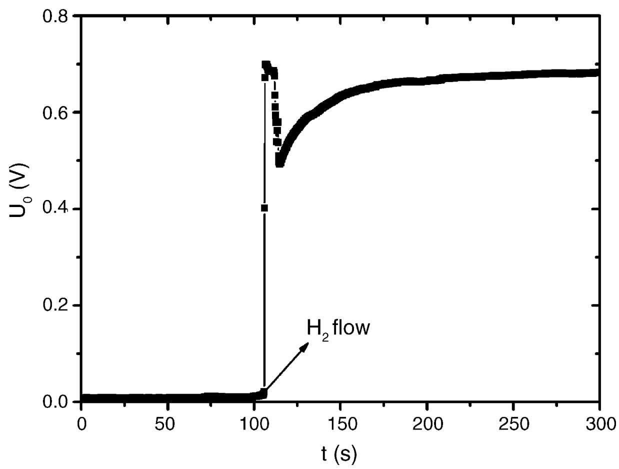

Fig. 4. Open circuit voltage behavior of the SOFC before, during and after anode hydrogen reduction at 600 °C.

For the electrical measurements, the single-cell is positioned in the test chamber. The first step is to connect the Pt leads and meshes to both electrodes and raise the temperature of the system to 800 °C for 30 min. At this temperature, a pyrex ring placed over the anode is partially melted, serving as sealant of the fuel chamber. The temperature of the system is slowly reduced to 600 °C and air is blown into the cathode chamber. After temperature stabilization, the in situ anode reduction was investigated by recording the electric potential U between cathode and anode, as shown in Fig. 4. With air flowing in both anode and cathode chambers of the test system, the single-cell open circuit voltage U_0 ~10 mV was found to be time independent. After ~100 s, H_2 was set to flow in the anode fuel chamber and an abrupt increase of the electric potential is observed (Fig. 4). Upon H_2 flow, the U_0 increases rapidly from 10 mV to ~0.7 V in ~5 s time interval, suggesting that the NiO reduction occurs very rapidly at 600 °C under H_2. In fact, as NiO is reduced, the open circuit voltage of the SOFC is reached, and the minimum H_2 flux necessary to maintain U_0 is stabilized at ~0.5 slpm. Under stable gas flow, U_0 remains constant after ~150 s and the temperature of the system were raised up to 700 °C at 5 °C min^{-1}. However, no significant dependence on the temperature was observed and U_0 was found to be ~0.7 V.

The results of open circuit voltage impedance spectroscopy measurements carried out at 700 and 800 °C are shown in Fig. 5. The impedance diagrams show an inductive parasite effect at high frequencies (f > 100 kHz), an artifact of the experimental setup. This parasite inductance was found to be nearly temperature independent and estimated to be ~5 μH [16]. An equivalent circuit model, consisting of a resistor R and two parallel resistor//constant phase element (R//CPE) circuits connected in series was used to fit the impedance data. The impedance diagrams exhibit a high frequency intercept (R_0), which is related to the electrolyte resistance, and two relaxations at lower frequencies. At intermediary and low frequency ranges, two

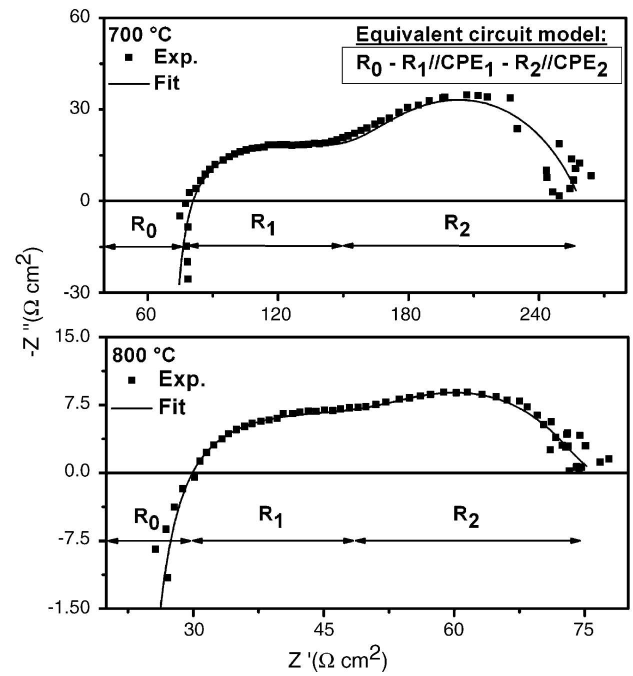

Fig. 5. Electrochemical impedance spectroscopy diagrams of the SOFC at 700 and 800 °C. The experimental and fitted diagrams are shown along with the schematic representations of three components of the equivalent circuit model (R_0, R_1 and R_2).

relaxations associated with the R_1//CPE_1 and R_2//CPE_2 components, respectively, are observed. These relaxations are possibly related to convoluted contributions arising from the electrolyte/electrode interfacial resistance and the electrochemical reactions taking place at the electrodes [13]. In fact, similar impedance diagrams have been reported: impedance measurements under different atmospheres on both the cathode and the anode revealed a correspondence between the lower frequency relaxation and the anode contribution [17,18]. Using the equivalent circuit model, the electrical resistance values R_0, R_1 and R_2 were estimated. Increasing the temperature from 700 to 800 °C results in the decrease of the total area specific resistance of the single-cell from ~32 to ~9.5 Ω cm^{-2}. The temperature evolution of the fitted components indicates that the activation energies associated with the R_0 and R_1 components are close to the ones of the YSZ solid electrolyte. On the contrary, the relative decrease of the component R_2 at 800 °C suggests that this contribution has higher activation energy, probably being the rate determining step reaction at the electrodes.

The current–voltage (I–V) curves of the SOFC single-cells, displayed in Fig. 6, were taken at 700 and 800 °C after the corresponding impedance measurements. In addition, the polarization curve at 700 °C was measured after ~2 h under operation at 800 °C to check the stability of the SOFC.

The I–V plots are linear indicating that the main loss mechanism is related to the ohmic polarization of electrodes and electrolyte. In fact, the characteristic features of both activation and diffusion polarizations usually observed in the

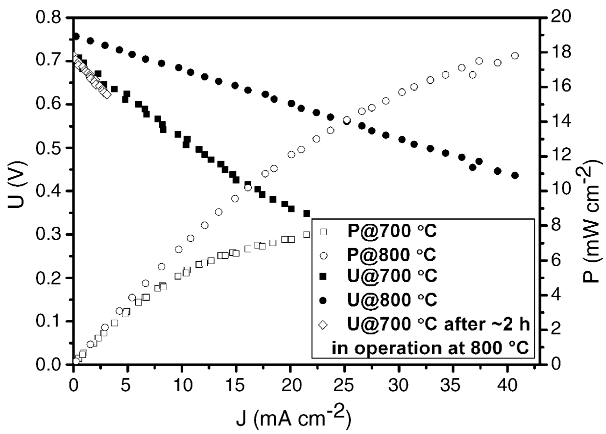

Fig. 6. *I–V* and power density curves of a single SOFC measured under flowing hydrogen in the anode and air in the cathode at 700 and 800 °C, and 700 °C after ∼2 h under operation at 800 °C.

I–V plots of fuel cells were found to be absent in the investigated current range. The peak power densities measured at 700 and 800 °C were ∼7 and ∼18 mW cm^{-2}, respectively.

Both *I–V* measurements at 700 °C yield the same data, an indication of the good stability of the system in the investigated electrical current range (Fig. 6). The U_0 values at 700 °C measured before and after the operation at 800 °C for 2 h were found to be approximately the same of the one at 600 °C (∼0.7 V). However, the increase of the temperature to 800 °C leads to an increase in U_0 to ∼0.75 V. The U_0 values are below the expected thermodynamic potential for the H_2 oxidation reaction in a SOFC [19]. The observed difference may be associated with electrical resistances arising from the electrical contacts as well as internal electrical resistances of the single-cell. The area specific ohmic resistances determined from the polarization curves are ∼8 and ∼17 Ω cm^{-2} at 800 and 700 °C, respectively. These values correspond to the sum of the impedance components at high and intermediary frequencies $R_0 + R_1 = 7$ and 19 Ω cm^{-2} at 800 and 700 °C, respectively.

The combined results suggest that the relaxation at intermediary frequencies in the impedance diagrams is associated with ohmic resistances that are possibly related to contact resistances at the electrolyte/electrode interfaces [20]. In addition, both power density and U_0 values are strongly influenced by the observed microstructural features of the single SOFC (Fig. 3). The relatively high area specific resistance and the ohmic polarization observed in the electrical measurements performed at moderate temperatures are probably related to both the anode low porosity and the electrolyte thickness [1]. An optimized porous microstructure of the anode support and a thinner electrolyte layer may contribute to the performance of the cell. The *I–V* curves and the impedance diagrams at the lower frequency range suggest that pore formation due to NiO reduction (∼15 vol.%) is insufficient for the maximization of the triple phase boundary length in the anode.

4. Conclusions

The slurry-coating method was used for the deposition of thin electrolyte and composite cathode layers for preparing anode-supported single SOFCs. The electrochemical measurements allowed for the characterization of the single-cells, revealing that the anode reduction occurs very rapidly at 600 °C under H_2 flow. In addition, the main loss mechanism observed in the electrical properties of the SOFC is due to ohmic resistances, which are probably associated with the electrolyte thickness and contact resistances of the electrolyte/electrode interfaces. Emphasis was given to the use of raw materials found in Brazil, yttria-stabilized zirconia and lanthanum oxide. To the best of our knowledge, this is the first report of a successful SOFC experiment in Brazil. The results indicate that with appropriate powder synthesis and fabrication processes, further developments may be useful for economic viable fabrication of SOFCs capable of improved high current output. In particular, pore former addition to the anode support, improved electrolyte thickness control, and new materials for moderate temperature operation are being developed [20–22]. In addition, ethanol is being considered as a competitive fuel for powering the SOFCs.

Acknowledgements

To CNEN, PRONEX, FAPESP (99/10798-0, 98/14324-0, 03/08793-8) and CNPq (401051/03-0, 306496/88, 300934/94-7, 301661/04-9) for financial support and scholarships.

References

[1] B.C.H. Steele, A. Heinzel, Nature 414 (2001) 345–352.
[2] N.Q. Minh, Solid State Ionics 174 (2004) 271–277.
[3] N.Q. Minh, J. Am. Ceram. Soc. 76 (1993) 563–588.
[4] H. Yakabe, Y. Baba, T. Sakurai, Y. Yoshitaka, J. Power Sources 135 (2004) 9–16.
[5] S. Primdahl, M.J. Jorgensen, C. Bagger, B. Kindl, Proceedings of Solid Oxide Fuel Cells VI, 1999, p. 793.
[6] J.P. Ouweltjes, F.P.F. van Berkel, P. Nammensma, G.M. Christie, Proceedings of Solid Oxide Fuel Cells VI, 1999, p. 803.
[7] D. Stover, U. Diekmann, U. Flesch, H. Kabs, W.J. Quadakkers, F. Tietz, I.C. Vinke, Proceedings of Solid Oxide Fuel Cells VI, 1999, p. 812.
[8] J.W. Stevenson, P. Singh, Abstracts of Fuel Cell Seminar, 2002, p. 890.
[9] Global Thermoelectric Inc., Abstracts of Fuel Cell Seminar, 2002, p. 974.
[10] K.C. Wincewicz, J.S. Cooper, J. Power Sources 140 (2005) 280–296.
[11] E.C. Subarao, Advances in Ceramics, in: A.H. Heuer, L.W. Hobbs (Eds.), Science and Technology of Zirconia, vol. 3, The Am. Ceram. Soc. Inc., Columbus, 1981, pp. 1–24.
[12] S. Geiger, Fuel Cells in Brazil a Survey of Current Developments, Fuel Cell Today, 26 March 2003, pp. 1–9.
[13] S.P. Jiang, J.G. Love, Y. Ramprakash, J. Power Sources 110 (2002) 201–208.
[14] E.N.S. Muccillo, R. Muccillo, Br. Ceram. Trans. 101 (2002) 259–262.

[15] P. Duran, J. Tartaj, F. Capel, C. Moure, J. Eur. Ceram. Soc. 23 (2003) 2125–2133.
[16] D.Z. de Florio, V. Esposito, G. Savo, E. Di Bartolomeo, E. Traversa, Proceedings of Solid Oxide Fuel Cells VIII, 2003, p. 488.
[17] B.W. Chung, C.N. Chervin, J.J. Haslam, A.-Q. Pham, R.S. Glass, J. Electrochem. Soc. 152 (2005) 265–269.
[18] T. Tsai, S.A. Barnett, Solid State Ionics 93 (1997) 207–217.
[19] V. Ramani, H.R. Kunz, J.M. Fenton, Interface 13 (2004) 17.
[20] D.Z. De Florio, R. Muccillo, V. Esposito, E. Di Bartolomeo, E. Traversa, J. Electrochem. Soc. 152 (2005) 88–92.
[21] S.K. Tadokoro, T.C. Porfirio, R. Muccillo, E.N.S. Muccillo, J. Power Sources 130 (2004) 15–21.
[22] V. Esposito, D.Z. de Florio, F.C. Fonseca, E.N.S. Muccillo, R. Muccillo, E. Traversa, J. Eur. Ceram. Soc. 25 (2005) 2637–2641.